



HAL
open science

Impact of the genetic-environment interaction on the dynamic of nitrogen pools in arabidopsis

Giorgiana Chietera, Sylvain S. Chaillou, Magali Bedu, Anne Marmagne, Céline Masclaux-Daubresse, Fabien Chardon

► To cite this version:

Giorgiana Chietera, Sylvain S. Chaillou, Magali Bedu, Anne Marmagne, Céline Masclaux-Daubresse, et al.. Impact of the genetic-environment interaction on the dynamic of nitrogen pools in arabidopsis. Agriculture, 2018, 8 (2), pp.1-19. 10.3390/agriculture8020028 . hal-02623578

HAL Id: hal-02623578

<https://hal.inrae.fr/hal-02623578>

Submitted on 26 May 2020

HAL is a multi-disciplinary open access archive for the deposit and dissemination of scientific research documents, whether they are published or not. The documents may come from teaching and research institutions in France or abroad, or from public or private research centers.


L'archive ouverte pluridisciplinaire **HAL**, est destinée au dépôt et à la diffusion de documents scientifiques de niveau recherche, publiés ou non, émanant des établissements d'enseignement et de recherche français ou étrangers, des laboratoires publics ou privés.



Distributed under a Creative Commons Attribution 4.0 International License

Article

Impact of the Genetic–Environment Interaction on the Dynamic of Nitrogen Pools in *Arabidopsis*

Giorgiana Chietera ¹, Sylvain Chaillou ¹, Magali Bedu ^{1,2}, Anne Marmagne ¹,
Céline Masclaux-Daubresse ¹ and Fabien Chardon ^{1,*} 

¹ Institut Jean-Pierre Bourgin, INRA, AgroParisTech, CNRS, Université Paris-Saclay, 78000 Versailles, France; giorgiana.chietera@genmils.com (G.C.); sylvain.chaillou1@gmail.com (S.C.); magali.bedu@agroparistech.fr (M.B.); anne.marmagne@inra.fr (A.M.); celine.masclaux-daubresse@inra.fr (C.M.-D.)

² AgroParisTech, UMR GENIAL, 1 Avenue des Olympiades, 91744 MASSY CEDEX, France

* Correspondence: fabien.chardon@inra.fr; Tel.: +33-1-30-83-33-76

Received: 15 December 2017; Accepted: 12 February 2018; Published: 14 February 2018

Abstract: Mineral nutrient availability and in particular nitrogen abundance has a huge impact on plant fitness and yield, so that plants have developed sophisticated adaptive mechanisms to cope with environmental fluctuations. The vast natural variation existing among the individuals of a single species constitutes a great potential to decipher complex traits such as nutrient use efficiency. By using natural accessions of *Arabidopsis thaliana* that differ for their pattern of adaptation to nitrogen stress, we investigated the plant response to nitrate supplies ranging from 0.01 mM up to 50 mM nitrate. The biomass allocation and the different nitrogen pools in shoot and in roots were monitored to establish the nutrition status of each plant. Analysis of variation for these traits revealed genetic differences between accessions for their sensibility to nitrate availability and for their capacity to produce shoot biomass with the same nitrogen nutrition index. From the correlation matrix of all traits measured, a statistical model was formulated to predict the shoot projected area from the nitrate supply. The proposed model points out the importance of genetic variation with respect to the correlation between root thickness and amino acids content in roots. The model provides potential new targets in plant breeding for nitrogen use efficiency.

Keywords: nitrogen use efficiency; G × E interaction; natural variation; nitrogen stress; *Arabidopsis thaliana*

1. Introduction

In addition to light, water and temperature, mineral nutrient availability has a huge impact on plant growth and fitness, and in an agricultural context, on crop yield. As sessile organisms, plants cannot escape unfavorable atmospheric or edaphic conditions; therefore, they have developed sophisticated adaptive mechanisms allowing them to cope with the dramatic fluctuations of their environment. This is particularly well illustrated by the strategic acquisition of mineral nutrients from the soil by the roots. For instance, the availability of nitrate (NO₃), the main nitrogen (N) source for nutrition in most high plant species, can vary dramatically in both time and space. Plants are able to react to these variations thanks to specific NO₃ sensing systems, making this ion one of the most potent signal molecule affecting plant physiology and development [1]. The biochemical mechanisms involved in NO₃ uptake, assimilation and remobilization have been widely studied in order to identify the features that determine the nitrogen use efficiency (NUE) of a plant [2–6]. The effect of low N availability on plant biomass, NO₃ uptake, ion contents and root architecture has been widely investigated [7–10]. There is evidence that plants modify their root architecture, changing the lateral to primary roots ratio and decreasing the shoot-to-root ratio at the same time, to forage the soil for

nutrients. This foraging response normally involves increased proliferation of lateral roots within nutrient-rich soil patches [11]. Genome-wide microarray analysis in the model plant *Arabidopsis thaliana* under limiting nitrogen conditions shows extensive changes in primary and secondary metabolisms, protein synthesis, and cellular growth processes, with numerous changes to regulatory genes and other cellular pathways [8]. The phenotypic description of Arabidopsis Recombinant Inbred Lines (RIL) built-up to study the plant response to low and high N supplies [12], identified multiple sources of physiological variation, such as those leading to the variations of shoot biomass, nitrogen percentage and free amino-acids content [13]. Several studies showed decreases in total N%, in NO₃ reserves and in total free amino-acids content in plants grown on low regimes [14–16], while soluble proteins content remains unchanged in rosettes [10]. On the other hand, rubisco degradation releases numerous free amino acids available for phloem loading and other interconversions in N depleted plants [2]. One possibility is that amino acids would be interconverted to increase the synthesis of amino acids dedicated to transport, such as glutamine and asparagine. It has also been proposed by Richard-Molard et al. [15] that the initial size of the N storage pool is crucial for the capacity of plants to cope with nitrate starvation, unlike the remobilization dynamics and the composition of the internal N pool [14]. The reduction of growth and photosynthesis, the remobilization of N from old, mature organs to actively growing ones, and the accumulation of abundant anthocyanins, have also been observed in N-starved plants [17]. The complexity of plant responses to temporary or chronic N depletion makes it difficult to give simple explanations, and very often results are contradictory, mainly because of different experimental conditions.

Among individuals belonging to the same plant species, there are great genetic variations for traits that contribute to NUE, including total N uptake, post-anthesis N uptake, N translocation from roots to shoot, and N assimilation [18]. Plant responsiveness to N availability depends on both genotype and the interaction of genotype with N supply level [19]. Root architecture plasticity traits have been investigated in *Arabidopsis* in relation to N availability by De Pessemier et al. [7]. This study, conducted on a core-collection of 24 accessions, together with the one conducted by Sulpice et al. [20] on 97 *Arabidopsis* accessions for biomass traits in response to carbon (C) and N nutrition, confirms that a large genetic variation exists in response to nutrient availability within the same species. Results point out the existence of a huge potential to elucidate complex traits such as NUE. Using a natural variation approach, several studies have been conducted in different species in order to individuate the most performing genotypes in response to nutrients availability [21]. Since *Arabidopsis* accessions have been found in a wide range of habitats differing notably in soil richness, this species constitutes a very suitable model for studying genetic variability of plant adaptation to nutrient availability [22]. Recent investigations on N perturbed environments have underlined some major differences between *Arabidopsis* accessions when they face N fluctuations [14,16]. In particular, Ikram et al. [16] identified accessions showing contrasted responses and different growth adaptive strategies using a core-collection of 23 accessions. Thanks to the comparison of N-limited and N-starved plants to control ones, it was possible to differentiate the adaptive responses of plants by highlighting master traits influencing growth under each nutritional condition. Moreover, it was possible to depict four distinct patterns of adaptation that exist among *Arabidopsis* accessions that allow the plants to tolerate the imbalance in exogenous N supply.

Despite the efforts to discover genes involved in NUE, few crop-breeding programs today include genomic selection [23]. The first limitation of the selection progress comes from the complexity of the genetic architecture of the NUE process. The second limitation is the existence of a strong genotype \times environment interaction (G \times E) that modulates the number of key genes and their interactions in the network controlling the process. These G \times E interactions require considerable experimental effort to identify the persistent traits that contribute to NUE increases across many environments. Computer-based modelling approaches have recently emerged as a method to save time, labor, and resources, and to infer trait values beyond field experiments [24]. Early models focused on leaf to canopy assimilation, with emphasis on light interception and canopy architecture [25].

Subsequent modelling efforts progressed to develop whole crop models where life cycle prediction, life-long C balance and growth of different organs were emphasized. For example, this has been done for phenological development in soybean [26], leaf elongation rate in maize [27], or fruit quality in peach [28]. All of these studies pointed out the necessity for linking model parameters with easily measurable physiological traits [29]. Among the processes that are needed for improving plants models, Boote et al. [25] highlight the importance of mechanistic methods for predicting allocation of C and N assimilates among plant organs and a better linkage to soil nutrients and soil fertility. An eco-physiological model simulating relations between leaf area and root N retrieval has been developed in *Medicago truncatula* [30], another pointed out the relationship between yield-related traits, N uptake and assimilates with drought stress in rice [31], while in wheat, nine nitrogen treatments have been put in correlation with the grain protein composition [32].

In our study, we investigate the Genotype by Nutrition interaction by describing responses of four *Arabidopsis* accessions to six different N environments. We first characterize the plant response to N stress following variations of the morphological and metabolic traits measured both in shoot and roots. We then present an integrated genetic and physiological model obtained from the investigation of important traits related to N nutrition management in *Arabidopsis*, thanks to the description of the responses of four contrasted accessions to six different N environments. The proposed model allows the prediction of relevant biomass values from the environmental N availability thanks to strong correlations between different metabolic and morphological traits. The model can moreover lead to a predictive description of the principal entities that respond to N stress environment as well as to estimate the main variations among accessions that might explain differences in their NUE.

2. Materials and Methods

2.1. Selection of Accessions

Each one of the accessions used in this study, *Bur-0*, *Col-0*, *Cvi-0*, and *Ge-0*, belongs to one of the four classes described in Ikram et al. [16]. They are therefore characterized by contrasted responses to an N-perturbed environment. Seeds were obtained from a Versailles stock center (<http://publiclines.versailles.inra.fr/>).

2.2. Growth Conditions and Experimental Design

Seeds were surface-sterilized by using ethanol-'bayrochlor' (95–5% *v/v*) and shaken in this solution shaken for 8 min, then they were rinsed in clear sterile water and allowed to dry. Sowing was done using a toothpick, placing two seeds on the top of one cut Eppendorf tube filled with 0.7% agar and inserted into 96-wells trays filled with distilled water. Seeds were then stratified at 4 °C for three days before transfer to the growth chamber. Growth chamber conditions were as follows: short-day photoperiod of 8 h light at 21 °C, and 16 h darkness at 17 °C, 150 $\mu\text{mol m}^{-2} \text{s}^{-1}$ photon flux density and relative humidity was 65%. On the seventh day of growth, seedlings were transferred to six black plastic tanks (1 tank per nutrition) each one hosting 54 plants in a 6 × 9 grid. Each genotype was represented by 12 plants per nutrition regime that were harvested by groups of three to form four biological replicates. Spare holes were filled with additional plants in order to dispose of the highest number of homogeneous plants to compose replicates at harvest. Plastic tanks were filled with 15 L of nutrient solution. The whole set of plants was grown in complete nutrient solution (4 mM NO_3) until the 21st day after sowing (das) in order to give them a common background and to allow the formation of N initial stock, then split onto 6 different NO_3 regimes for a 14 day period (up to harvest). Solutions were renewed once a week. Nutrition regimes contained respectively NO_3 at a concentration of 0.01 mM, 0.2 mM, 1 mM, 4 mM, 10 mM, and 50 mM. One set of plants constituted a control group, since it was grown always at 4 mM NO_3 during the whole experiment. Hydroponic culture lasted 35 days in total, in which all plants remained in vegetative stage. Shoots and roots of each plant were separated at harvest. Roots were measured for primary root length and patted dry with a paper towel

before weighting. Root thickness values were obtained by simply dividing root weight by primary root length. After weighing, shoots and roots were frozen in liquid nitrogen. The same experimental culture was repeated three times and collected samples were stored at $-80\text{ }^{\circ}\text{C}$ until the metabolite extraction procedure.

2.3. Composition of Solutions

Complete nutrient solution contained 4mM nitrate as a sole nitrogen source and it was composed as follows: 3 mM KNO_3 , 1.7 mM CaCl_2 , 2 mM MgSO_4 , 2 mM KH_2PO_4 , 1 mM K_2SO_4 , and 0.5 mM $\text{Ca}(\text{NO}_3)_2$. In 0.01 mM, 0.2 mM, and 1 mM NO_3 nutrition, only KNO_3 was present to constitute the desired N concentration. Deficits of potassium and calcium compared to the complete nutrition solution were compensated by using K_2SO_4 at a concentration of 2.5 mM, 2.4 mM, and 2 mM respectively, and CaCl_2 at a concentration of 2.2 mM. In 10 mM and 50 mM NO_3 solutions, KNO_3 was added at a concentration of 3 mM and 5 mM respectively, while $\text{Ca}(\text{NO}_3)_2$ was added at a concentration of 3 mM and 22.5 mM respectively. CaCl_2 was decreased to 0.3 mM in both solutions while K_2SO_4 was eliminated in 50 mM NO_3 solution. All nutrient solution contained microelements in the same amount as follows: 22 μM Na_2EDTA , 0.01 μM CoCl_2 , 0.9 μM CuSO_4 , 0.2 μM Na_2MoO_4 , 0.5 μM KI , and a solution of NaFeEDDHA in final concentration of $1\text{ mL}\cdot\text{L}^{-1}$.

2.4. Extraction of Metabolites

Samples were ground with the help of steel bullets in a shaking grinder, and an aliquot of the obtained powder was weighed and used for extraction of metabolites. A two-step ethanol–water extraction was used, as described in Loudet et al. [13]. The first step consisted in a 25-min extraction at $80\text{ }^{\circ}\text{C}$ using 500 μL of 80% (*v/v*) ethanol, whereas the second step completed the extraction by using 500 μL of double-distilled water at $80\text{ }^{\circ}\text{C}$ for 20 min. Supernatants obtained from the two extractions were collected and put together in a well of a 2 mL-96 well plate and dried overnight in a speed-vacuum machine. Samples were then dissolved in 600 μL of double-distilled water and frozen at $-20\text{ }^{\circ}\text{C}$ before analysis. Pellets obtained after removing supernatants were dried for one night at $40\text{ }^{\circ}\text{C}$ and used for starch extraction.

2.5. Starch Content

Pellets were mixed with 50 mM 3-(N-morpholino)propanesulfonic acid (MOPS) (pH 7) and an amylase solution (15 U) was added to each sample. Samples were incubated at a temperature of $100\text{ }^{\circ}\text{C}$ for 6 min. Later, amyloglucosidase (35 U) dissolved in 0.2 M sodium acetate (pH 4.8) was added. After agitation and incubation for 5 hours at a temperature of $50\text{ }^{\circ}\text{C}$, samples were spun for 10 min at 14,000 r/min. Supernatants were collected and conserved at $-20\text{ }^{\circ}\text{C}$ before dosage. Starch content was quantified from extracts using the Roche analysis kit, using glucose as a standard. The results were expressed in nmol/mg of dry matter.

2.6. Nitrate Content

Extracts were evaporated and diluted in water before analysing them for nitrate contents. The method used was as described by Miranda et al. [33]. The reactant was prepared by dissolving vanadium III chloride (0.5 g), *N*-(1-naphthyl)ethylenediamine (0.01 g), and sulphanilamide (0.2 g) in HCl (0.5M); 1 mM NaNO_3 was used as standard. After loading the plate with samples (100 μL), an equal volume of reactant was added to each well and the reaction was carried out at room temperature for 5–6 h. The absorbance at 540 nm was measured using a spectrophotometer (Labsystem iEMS Reader MF) and used to estimate the nitrate content in nmol mg^{-1} dry matter (DM).

2.7. Amino Acids Content

The same extracts were subjected to an evaluation of free amino acid content using glutamine as a standard Rosen [34]. Briefly, ninhydrin colour reagent was first made by dissolving 0.3 g of ninhydrin (Sigma-Aldrich Chimie, Lyon, France) in 10 mL of methyl cellosolve (Sigma-Aldrich Chimie, Lyon, France). Cyanide acetate reagent was then prepared by mixing Na-acetate buffer (25 mL, 2.5 M, pH 5.2) with the KCN (10 mM) solution 2/100 (*v/v*) just prior to reaction. In a 96-well (2 mL) plate containing 200 μ L of sample (diluted), 100 μ L of ninhydrin colour reagent followed by 100 μ L of cyanide acetate reagent were added. The plate was shaken and heated for 15 min at 100 °C. After cooling, 1 mL of isopropanol (50% *v/v*) was added to the wells of the plate and mixed well. Absorbance was read at 570 nm on a spectrophotometer. This result was used to calculate the amino acid content in nmol mg⁻¹ DM using a glutamine 4 mM dilution set as calibration standard.

2.8. Ammonium Content

Ammonium was determined adding a solution of 2% 5-sulfosalicylic acid according to the Berthelot method to samples extracted in a hydro-alcoholic procedure as previously described. Calibration curve was obtained using a 1 mM (NH₄)₂SO₄ dilution series.

2.9. Nitrogen and Carbon Percentage

N% and C% were determined using lyophilized plant powder (1 mg) and the Dumas combustion method with an NA1500CN Fisons instrument (Thermoquest, Runcorn, Cheshire, UK) analyzer.

2.10. Soluble Proteins Content

Soluble proteins were extracted from 30 mg of fresh shoots material, and ground in a shaker with Eppendorf safe-lock 2 mL tubes. In each tube, one spatula of Fontainebleau sand was added to plant material in order to facilitate a homogeneous grinding procedure, together with 250 μ L of buffer composed as follows: 250 mM Tris HCl at pH 7.6, 10 mM Na-EDTA, 10 mM MgCl₂, 28.6 μ M β -mercaptoethanol and 2 μ M leupeptine. Tubes were kept at low temperature by cooling them in liquid nitrogen before the grinding process and keeping them on ice afterward. After extraction, samples were centrifuged and 200 μ L from each tube were transferred to a 96-well plate which was then stored at -20 °C. Protein concentration was determined using a commercially available kit (Coomassie Protein assay reagent, BioRad, Hercules, CA, USA) and bovine serum albumin (BSA) as a standard.

2.11. Shoot Projected Area

The shoot projected area was obtained by area calculation of rosettes pictures of each genotype, with the software ImageJ (<https://imagej.nih.gov/ij/index.html>); the selected surface area was then divided by the number of plants grown in the same tank to give an average estimation for a single plant.

2.12. Determination of Nc and Nutrition Indexes

Nc was obtained by choosing the average N% in shoots in plants growing at 4 mM. Nutrition indexes were calculated by the following formula usually used to compute the Nitrogen Nutrition Index (NNI) [35], but generalized to others N pools:

$$\text{Nutrition Index} = (\text{Pool}_{\text{observed}} \times \text{SFM}_{\text{observed}}) / (\text{Pool}_{\text{control}} \times \text{SFM}_{\text{control}})$$

where:

SFM_{control} is the shoot fresh matter (SFM) value at 4 mM NO₃,

SFM_{observed} is the SFM value observed,

Pool_{control} is the N pool value at 4 mM (N% for NNI, SAA and RAA for AANI, and SNO₃ and RNO₃ for NO₃NI),

Pool_{observed} is the N pool observed.

2.13. Statistical Analyses

Type III analysis of variance (ANOVA) analyses was carried out using XLSTAT. The ANOVA model for the phenotypical and metabolic data included three main effects (Genotype, Nutrition and Experiment) and the interactions combining all the effects. The ANOVA model for nutrition indexes included only the three main effects (Genotype, Nutrition and Experiment), the interaction effects were generally not significant. Effects were significant when the *p*-value was less than 0.001 for phenotypical and metabolic data and 0.05 for nutrition indexes.

The pairwise differences of slope of the linear regression of SFM against NNI among accessions were computed following the following adapted *T*-test:

$$T_{test} = \frac{(b_1 - b_2) / \sqrt{(n_1 + n_2 - 2)}}{\sqrt{SRR \cdot \left[\frac{1}{\sum_{n1} (NNI_{1,n1} - NNI_1)^2} + \frac{1}{\sum_{n2} (NNI_{2,n2} - NNI_2)^2} \right]}}$$

where:

b_1 is the slope of accession 1,

b_2 is the slope of accession 2,

n_1 and n_2 are the number of observation for the two accessions,

SSR is the sum of squared of the residuals,

NNI_1 is the average NNI of accession 1,

NNI_2 is the average NNI of accession 2,

$NNI_{1,n1}$ is the nth observed NNI of accession 1,

$NNI_{2,n2}$ is the nth average NNI of accession 2.

2.14. Statistical Modelling

Pairwise correlations between phenotypical and metabolic traits were calculated for all with a Pearson's correlation method. Correlation coefficients were tested for significance (*p* value < 0.01) by Excel spreadsheet at <http://www.stat-help.com/notes.html> with DeCoster utility for Applied Linear Regression [36]. For each correlation pair selected in the model, linear, logarithmic, and power regression were run on the whole data by using least squares methods in Excel spreadsheet. For each regression tested, the R-squared was recorded. Regression with the best R-squared was selected to fit the curve to the whole data. The same regressions were used on subsets concerning a single accession to fit the curve and determine the smooth parameters for the considered accessions.

3. Results

In order to investigate the effect of N environmental availability on Arabidopsis plants, six different supplies were tested with four accessions (*Bur-0*, *Col-0*, *Cvi-0* and *Ge-0*) belonging to different classes on the basis of their response to NO₃ nutrition [16]. All plants were grown at a control nutrition regime (4 mM NO₃) for three weeks, to give them a common background and to allow the formation of an initial N stock. Plants were then moved onto different N treatments. In nutritive solution, NO₃ was present at a concentration of 0.01 mM, 0.2 mM, 1 mM, 4 mM, 10 mM, and 50 mM. It constituted the only N source provided to the plants, which were harvested in their vegetative growth period, 35 days after sowing (das). The response to available N was evaluated by measuring 6 morphological and 13 metabolic traits at harvest, commonly used to give a description of the status of plants in nutritional studies [13,15,16,19]. The morphological traits were SFM, root fresh matter (RFM), the ratio between

shoot and roots fresh matter (SRFM), primary root length (RL), root thickness (RT), and the shoot projected area (SPA). The metabolic traits were shoot nitrate content (SNO3), roots nitrate content (RNO3), their ratio (SRNO3), shoot free amino-acids content (SAA), root free amino acid content (RNO3), their ratio (SRAA), total shoot carbon (C%), total shoot nitrate (N%), their ratio (C/N), shoot ammonium content (SNH4), root ammonium content (RNH4), shoot protein content (SPC), and shoot starch content (SStarch). All measurements were done on three independent and identical cultures. The raw data for the three cultures are in listed in Supplemental Table S1.

In order to determine the proportion of variance explained by genetic and environmental effects, ANOVA were performed for all studied traits under the six different nutrition regimes. Nutrition, accession (i.e., genotype), and culture (i.e., experiment) were considered as the main effects with potential interactions. ANOVA results are shown in Figure 1 and the proportion of explained variance for each effect are listed in Supplemental Table S2. Genotype has a significant impact on the variance of all the investigated traits, even when the percentage of explained variance was weak (Supplemental Table S2), except for N%. Morphological traits variation were confirmed to be mainly driven by genotype constraints, as already stated in Ikram et al. [16], with only one exception for SRFM whose variation was affected mainly by nutrition (40% of explained variation). Nutrition explained most of the variation for all metabolite traits, with a different percentage of explained variation depending upon each trait. However, RNH4 and SRAA were two exceptions, in which genotype effect has a higher impact than nutrition effect on the observed variation. ANOVA results indicated that metabolite traits were more affected by N status than by the genetic origin of accessions.

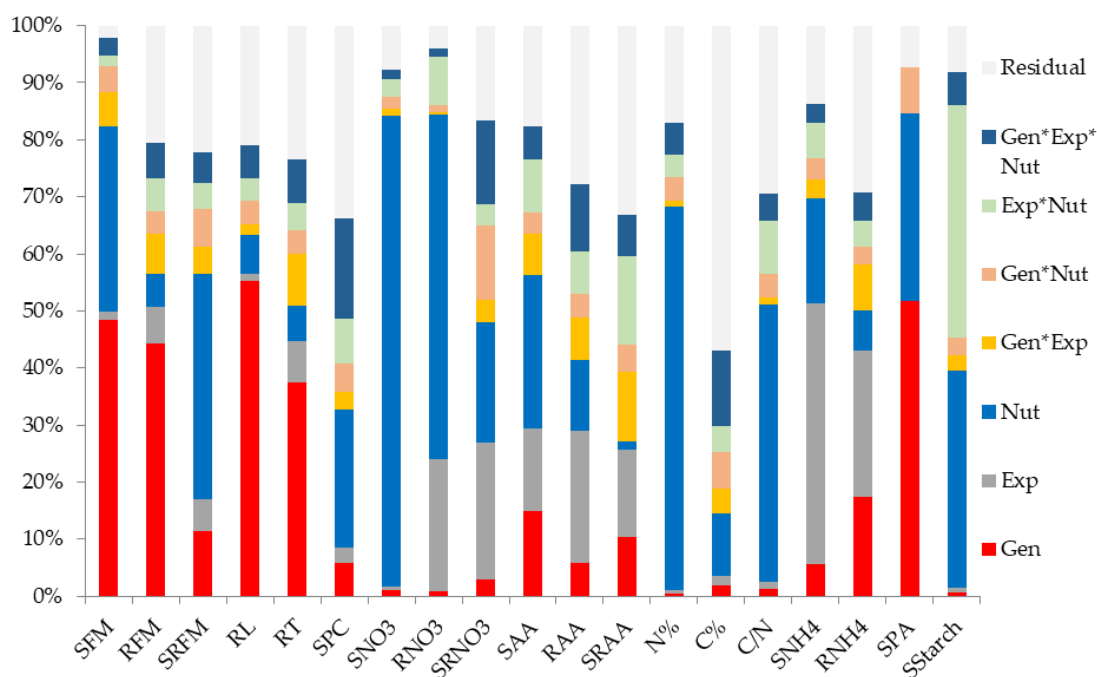


Figure 1. ANOVA of six morphological and 13 metabolic traits in four *Arabidopsis* accessions cultivated on six different nutrient supplies in three independent experiments. The morphological traits are: shoot fresh matter (SFM), roots fresh matter (RFM), shoot-to-root fresh matter ratio (SRFM), primary root length (RL) and root thickness (RT). The metabolic traits are: shoot protein content (SPC), shoot nitrate content (SNO3), roots nitrate content (RNO3), shoot-to-root nitrate content ratio (SRNO3), shoot amino acids content (SAA), roots amino acids content (RAA), shoot-to-root amino acids content ratio (SRAA), total nitrogen percentage (N%), total carbon percentage (C%), carbon to nitrogen percentages ratio (C/N), shoot ammonium content (SNH4), roots ammonium content (RNH4), shoot projected area (SPA) and shoot starch content (SStarch). Histograms show the effects due to: genotype (Gen), experiment (Exp), nutrition (Nut), interactions and residual (Residual), as percentages of the total variation.

3.1. Global Response of Arabidopsis Plants to a WIDE Range of NO₃ Supplies

The average morphological traits on the four accessions among the six nutrient regimes are presented in Figure 2.

SFM and SPA, two highly correlated traits ($r^2 = 0.88$), responded negatively to the extreme N supplies, both decreasing for the lowest as well as for the highest NO₃ concentrations (Figure 2A,B). SRFM showed the highest values at 4 mM, 10 mM, and 50 mM (Figure 2C). For root-related traits, responses to nitrate availability were the opposite of the responses of shoot-related traits. RFM showed the highest levels at low N (0.01 mM, 0.2 mM and 1 mM) and control (4 mM) conditions, while the lowest RFM were observed at 10 mM and 50 mM NO₃ (Figure 2D). RT showed medium values in the control condition (4 mM), with a significantly increased and decreased level in the lowest and in the highest NO₃ supplies respectively (Figure 2E). RL was at its maximum in the control condition (4 mM). It fell with decreasing NO₃ concentration in the media, with a significant change detectable at 0.01 mM as well as at 10 mM and 50 mM supplies (Figure 2F).

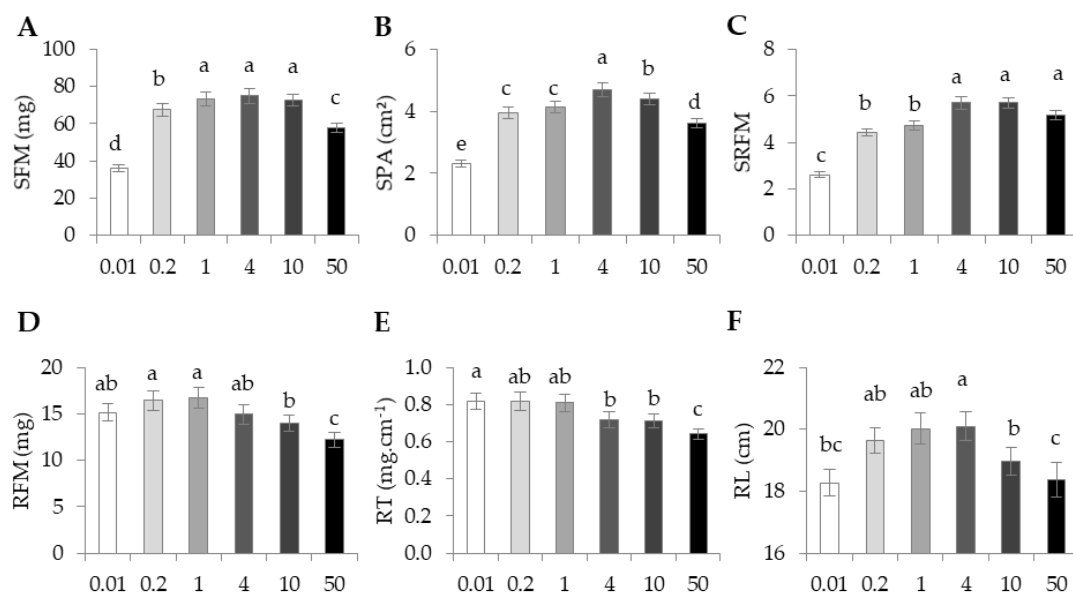


Figure 2. Average of morphological traits on the four Arabidopsis accessions grown in six different NO₃ supplies. On the x axis, nutrition regimes are reported in bars of different shades of grey, according to NO₃ concentration (mM). On the y axis, shoot fresh matter ((A)-SFM), shoot projected area ((B)-SPA), shoot-to-root fresh matter ratio ((C)-SRFM), root fresh matter ((D)-RFM), root thickness ((E)-RT) and primary root length ((F)-RL) are reported. Different letters indicate values that are significantly different at $p < 0.05$.

Average Arabidopsis metabolic traits for the six nutrition regimes are reported in Figure 3. By far, metabolic traits had a larger percentage of variation explained by nutrition compared to morphological traits (Figure 1). Interestingly, SNO₃, RNO₃, SAA, RAA, SNH₄, and RNH₄ steadily increased following the increase of NO₃ in solution (Figure 3A–F). This was also observed for N% from 0.01 mM, but it remained fairly constant between 0.2 mM and 50 mM (Figure 3G). C% had average values in the control condition with significantly higher and lower values at 0.01 mM and 50 mM respectively (Figure 3H). SPC showed a different trend in which the highest content was found at 1 mM and a gradual, but significant, decrease was observed at higher N supplies and at 0.01 mM (Figure 3L). The C/N ratio did not vary significantly except at 0.01 (Figure 3I). The nitrate ratio SRNO₃ remained stable in supplies between 1 mM to 50 mM, but it increased at supplies below 1 mM (Figure 3J). In contrast, the amino acid ratio SRAA remained constant in all conditions (Figure 3K). The average starch contents in shoot were higher than in the control condition in extreme supplies, at 0.01 mM and 50 mM (Figure 3M).

Beyond the potential offered by genotype for further investigations, a $G \times E$ interaction represented the specific genetic response to perturbed N environment. This was a significant source of variation for all the investigated traits to different extents, as SRNO3 and SRFM explained variations of 15.6% and 8.5% respectively (Supplemental Table S2).

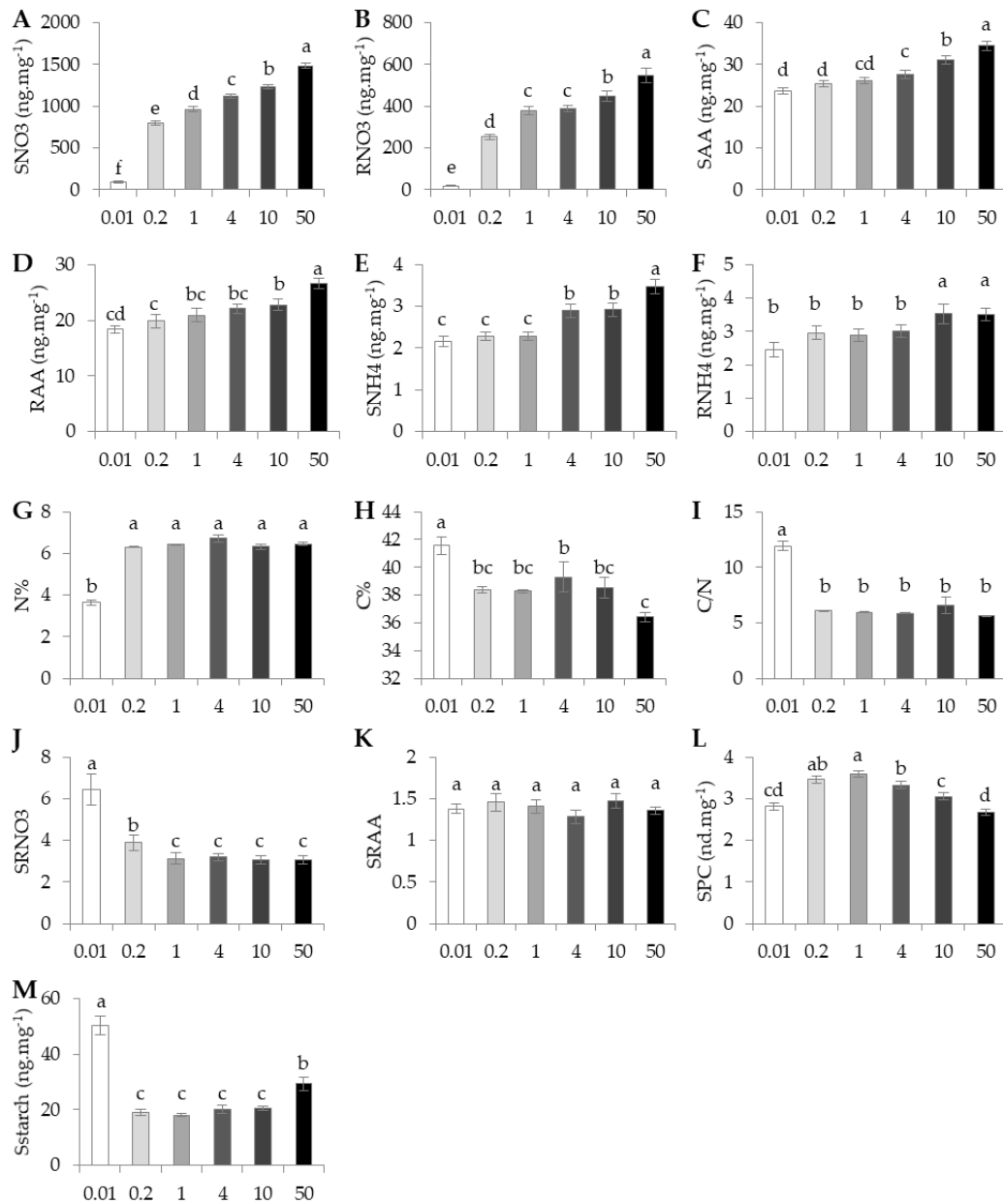


Figure 3. Average of metabolic traits on four *Arabidopsis* accessions grown in six different NO₃ supplies. On the x axis nutrition regimes are reported in bars of different shades of grey, according to NO₃ concentration (mM). On y axis are reported shoot nitrate ((A)-SNO3), roots nitrate ((B)-RNO3), shoot amino acids ((C)-SAA), roots amino acids ((D)-RAA), shoot ammonium ((E)-SNH₄), roots ammonium ((F)-RNH₄), nitrogen percentage ((G)-N%), carbon percentage ((H)-C%), carbon to nitrogen percentages ratio ((I)-C/N), shoot-to-root nitrate ratio ((J)-SRNO3), shoot-to-root amino acids ratio ((K)-SRAA), shoot protein content ((L)-SPC) and shoot starch ((M)-Sstarch). Different letters indicate values significantly different at $p < 0.05$.

The average *Arabidopsis* variation for SRNO3 showed the highest value at 0.01 mM NO₃, an intermediate value at 0.2 mM, and lower ones from 1 mM to 50 mM. This general trend was observed

in *Bur-0* and *Cvi-0* (Figure 4A). In *Col-0*, SRNO₃ remained steady for any nutrition regime and SRNO₃ varied significantly only for the two extreme NO₃ supplies (0.01 mM and 50 mM) in *Ge-0*. Among the morphological traits, SRFM showed the highest variation driven by G × E interaction (6% of explained variation). For *Bur-0* and *Cvi-0*, SRFM decreased significantly only at 0.01 mM, whereas in the two last accessions, SRFM was significantly different among low N conditions (0.01 mM, 0.2 mM and 1 mM) compared to high N conditions (4 mM, 10 mM and 50 mM, Figure 4B).

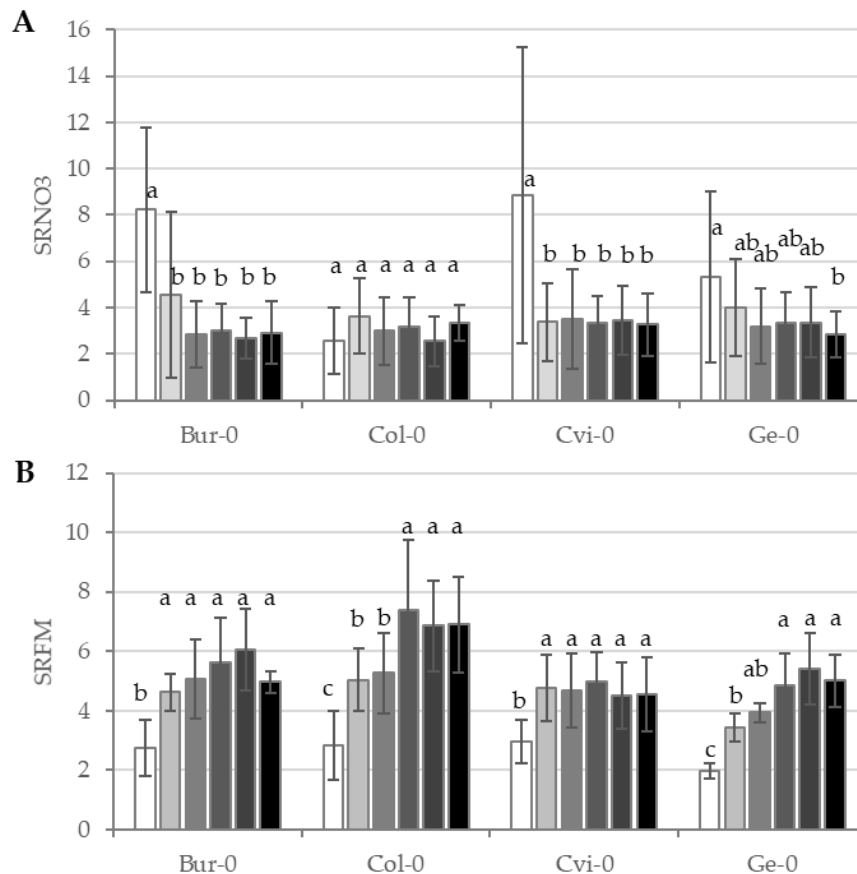


Figure 4. Genotype by nutrition interaction on trait variation. Shoot-to-root NO₃ content ratio ((A)-SRNO₃) and shoot-to-root fresh matter ratio ((B)-SRFM). The six different NO₃ supplies are reported in bars of different shades of grey. Different letters indicate values significantly different at $p < 0.05$.

3.2. Genetic Response to N Stress Environment

When we investigated morphological traits in the different conditions compared to the control at 4 mM, we distinguished clear differences among the 4 investigated accessions. A synthesis of the response of accessions to nutritional change compared to the control condition together with a plot for the average response are shown in Figure 5.

Compared to the situation at 4 mM, SFM and RFM decreased when plants were grown in other supplies in *Bur-0*, *Col-0*, and *Ge-0*, but the two traits increased in *Cvi-0* at 0.2 mM and 1 mM. *Col-0* showed a greater reduction of shoots and roots compared to *Bur-0* and *Ge-0*. These results suggested that *Cvi-0* was the most adapted accession to low N supplies, whereas *Col-0* was the accession the most sensitive accession to N fluctuation. The dramatic sensitivity of *Col-0* was observable on its root architecture. RL was reduced between -10% and -31% in the different N supplies for *Col-0*, whereas RL varied between 4% and -17% in others accessions. Interestingly, *Bur-0* did not show any significant difference for RL compared to the control condition. SRFM, the morphological trait for which the highest impact of G × E interaction was found, tended to decrease for all accessions in N

concentrations lower than the control, reaching significantly lower values at 0.01 mM, 0.2 mM, and 1 mM NO_3 for *Col-0* and *Ge-0*, while only at 0.01 mM NO_3 for *Bur-0* and *Cvi-0*. Among metabolic traits, we observed similarly various responses to N environment among accessions. For instance, SAA increased at 50 mM compared to the control condition (4 mM), but this trend was lower in *Col-0* compared to the other accessions (+12% in *Col-0* and +25% in average for the others). We noticed a great reduction of SAA in *Ge-0* at 0.01 mM although the reduction was weaker for the 3 other accessions (−26% for *Ge-0* and on average −0.14% for the others). At the roots level, the amino acids tended to increase with NO_3 availability (Figure 3E). However, RNO₃ was higher in all N conditions compared to the control condition in *Col-0* whereas in the three other accessions RNO₃ was reduced in low N conditions (0.01 mM, 0.2 mM and 1 mM) and increased at 50 mM. Compared to the control condition, SRNO₃ remained stable in other NO_3 conditions except at 0.01 mM where SRNO₃ increased for *Bur-0*, *Cvi-0*, and *Ge-0*. *Col-0* did not show any significant change at 0.01 mM NO_3 regime. These variations in the accession response to NO_3 availability suggested the existence of a natural variation for dynamics of nitrogen pools and sensitivity to external NO_3 concentration.

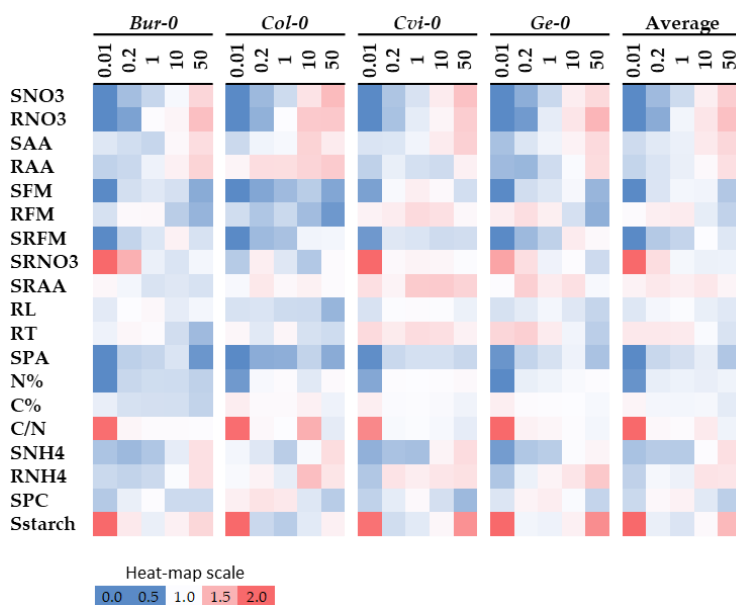


Figure 5. Heat-map of accession changes according to N fluctuations. Values measured in the different N condition are expressed as a ratio to control values (4 mM NO_3) for the four accessions (*Bur-0*, *Col-0*, *Cvi-0* and *Ge-0*) and for the total average (Average). Decreased and increased values in comparison to control are shown in blue and red shades, respectively.

Critical N concentration (N_c), i.e., the minimum N concentration in plants needed for the maximum growth rate [35], was estimated to be 6.4 N% in shoots for all accessions at the control condition (4 mM NO_3). N_c was stable at all N supplies above 0.2 mM NO_3 , but fell when plants were grown below this nitrate threshold. We then calculated the Nitrogen Nutrition Index (NNI) as the ratio between the amounts of N in plants growing in a specific supply compared to the N amount in plants growing in the control condition (Supplemental Table S3). This index allowed agronomists to diagnose nitrogen deficiency in crops [35]. NNI can vary from 0 in very deficient conditions, to values greater than 1 for ad lib consumption of N. The four studied accessions showed variation in their NNI under stress conditions (Figure 6A). *Cvi-0* seemed to have a good capacity to store N, since its NNI was greater than 1 when it grew between 1 mM and 10 mM NO_3 . We tested the effect of genotype on observed variation of NNI using an ANOVA with three main effects: genotype, nutrition, and experiment. The results of ANOVA, recorded in Supplemental Table S4, showed that the NNI of *Cvi-0* was significantly higher than the values of the three other accessions. For instance, the NNI of

Cvi-0 reached a maximum at 1 mM NO_3 . In contrast, the three other accessions always showed a NNI below 1 in conditions different from control (Figure 6A). At 0.01 mM, 38% of N present at the control condition (4 mM) was in *Cvi-0*, while other accessions had only between 22% and 27% of the N needed for the normal growth. In the same manner for NNI, we estimated the variation in the NO_3 pool and the amino acid pool respectively by calculating the nitrate nutrition index (NO3NI) and amino acids nutrition index (AANI—Supplemental Table S3). NO3NI is the ratio between the amounts of nitrate stored in plants growing in a particular supply, divided by the nitrate amount stored in plants growing at the control condition. AANI is the ratio between the amount of free amino acids in plants growing in particular supply divided by the amount stored in plants growing at the control condition, both in shoots and roots for each accession (Figure 6B–E). For the two nutrition indexes, *Cvi-0* showed significant higher indexes than the others accessions (supplementary Table S4). For instance, in shoot at 1 mM, around 75% of the nitrate pool and 80% of the free amino acid pool were filled for *Bur-0*, *Col-0* and *Ge-0* plants (NO3NI = 0.75 and AANI = 0.80) whereas the nitrate pool and the free amino acid pool in *Cvi-0* were optimal (NO3NI = 0.96 and AANI = 1.12, Figure 6B,C). Similarly, in roots at 0.02 mM, around 60% of the nitrate pool 70% of the free amino acid pool were filled for *Bur-0*, *Col-0*, and *Ge-0* plants (NO3NI = 0.54 and AANI = 0.71) whereas the nitrate pool and the free amino acid pool in *Cvi-0* were less reduced (NO3NI = 0.80 and AANI = 0.98, Figure 6D,E). The results suggested *Cvi-0* was less sensitive to NO_3 availability than the three other accessions since its pools of nitrogen remained full in N stress condition unlikely the common pattern in others accessions.

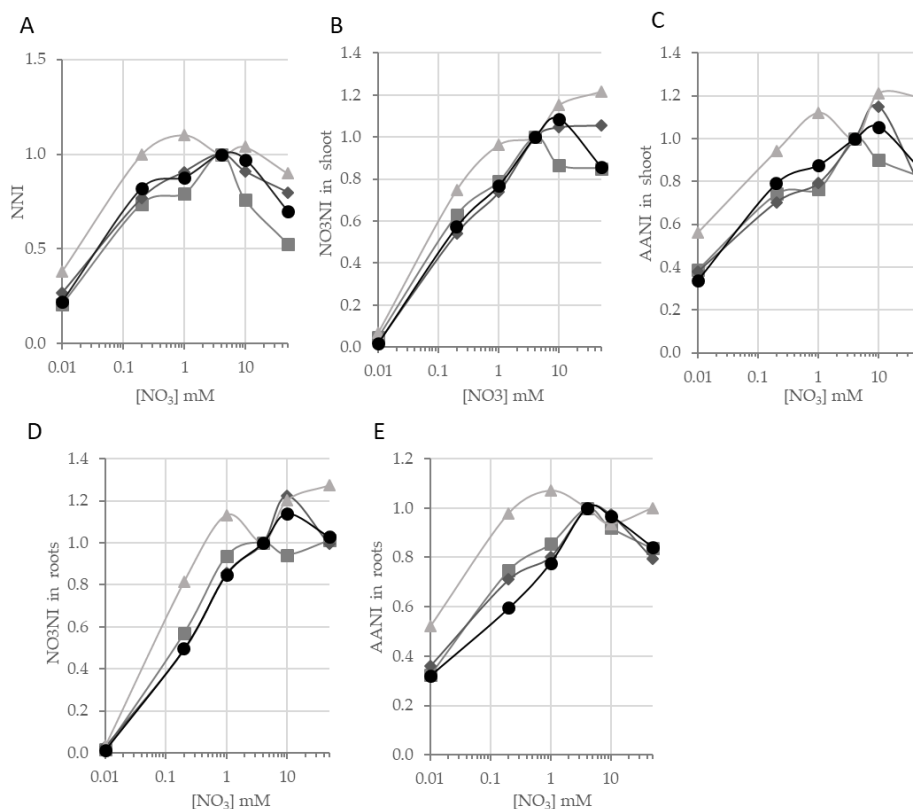


Figure 6. Nutrition Index of different N pools in four *Arabidopsis* accessions. On the y axis, Nitrogen Nutrition Index (NNI, (A), Nitrate Nutrition Index (NO3NI, (B) in shoot, (D) in roots) and Amino Acids Nutrition Index (AANI, (C) in shoot, (E) in roots) are reported, plotted against environmental NO_3 concentration on a logarithmic scale. Accessions are shown by squares, diamonds, triangles, and circles in different shades of grey for *Bur-0*, *Col-0*, *Cvi-0* and *Ge-0*, respectively.

To give an idea of natural variation for NUE, we plotted the SFM of each accession against their NNI (Figure 7). We observed a strong positive correlation between the two traits, suggesting a linear

response of plant growth to the N nutrition status in all accessions. However, the slopes of the linear regression line among accessions were significantly different among the four accessions (Supplemental Figure S1). These slopes allowed us to distinguish three groups of accession: *Bur-0* with the highest slope (77.6), *Cvi-0* and *Ge-0* with intermediate slopes (57.2 and 50.4, respectively) and *Col-0* with the lowest slope (28.8). Interestingly, we noticed that the order of efficiencies between accessions was the same when we considered the NO₃NI and AANI in the shoots (Supplemental Figure S2A,B). In contrast, the relationship between RFM and NO₃NI and AANI in roots was not linear (Supplemental Figure S2C,D). Taking together these results suggested that for a same nitrogen nutrition index, *Bur-0* was an efficient accession to produce shoot biomass whereas *Col-0* was an inefficient accession.

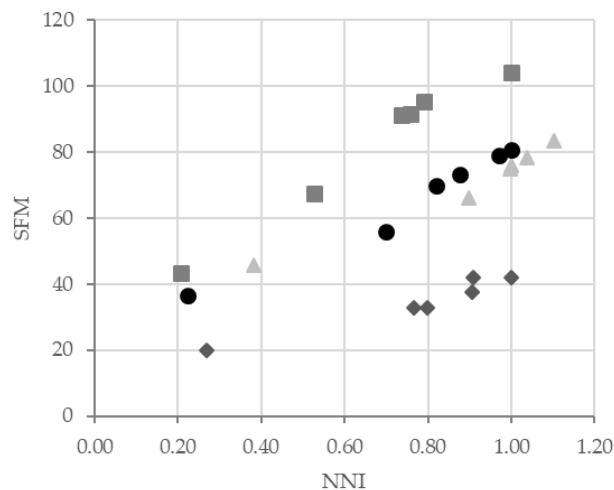


Figure 7. Nutrition Use Efficiency in four *Arabidopsis* accessions. Shoot fresh matter (SFM) of the four accessions are plotted against their Nitrogen Nutrition Index. Accessions are showed by squares, diamonds, triangles and circles in different shades of grey for *Bur-0*, *Col-0*, *Cvi-0*, and *Ge-0*, respectively.

3.3. Strong Correlations Drive the Construction of a Genetic-Physiologic Model of NUE in *Arabidopsis*

Because there was a strong genetic variation between plants, N nutrition did not correlate globally with easy-to-measure morphological traits such as SFM and SPA ($r^2 = -0.05$ and $r^2 = 0.01$, respectively). N nutrition only slightly correlated with RFM ($r^2 = -0.19$). It was thus not possible to predict plant biomass by only knowing the nutritional regime applied. Using Pearson's correlation matrix (Supplemental Table S5), we recorded the two highest correlations for each trait to build up a descriptive model starting from the traits that correlated with N nutrition the most, such as SNO₃ and RNO₃ ($r^2 = 0.60$ and $r^2 = 0.51$ respectively), towards biomass traits (Figure 8). Analyzing the correlation matrix, we identified four groups of traits corresponding to defined pools that were strongly correlated among them (Figure 8). The nitrate pools in shoot and roots were correlated directly to N regime. Traits linked to elements such as N% and C% followed the group of nitrate pools, and in particular SNO₃, by which they were linked by strong correlations. In a similar manner, a third group of traits related to amino acids and ammonium pools were well correlated to the group of nitrate pools. Lastly, traits related to biomass allocation, which includes SFM and RFM, were connected to the amino acids and ammonium pool, in view of the good correlation existing between RAA and RT ($r^2 = -0.61$). Interestingly, SPC represents a completely independent trait, showing weak correlations to others traits. From Figure 8, we drew the shorter pathway to connect the N nutrition of plants to SPA, in accordance to the arrow orientations. The model then consisted of six steps, connecting N nutrition to RNO₃, RAA, RT, RFM, SFM, and finally SPA (Table 1).

Plotting on x and y axis the observed values of traits that are linked by the black dotted line in Figure 8, we tested different equations to fit a regression curve to the whole data. For each step, we choose the curve that fit the better with the observed values, i.e., the highest R -squared value

(Table 1). Nutrition-RNO₃ and RAA-RT plots fitted with a logarithmic curve, RNO₃-RAA, RT-RFM, and SFM-SPA with a linear line, RFM-SFM with an exponential curve. Each parameter of these curves was first computed from the best fitted equation from all the available data (Table 1). We then estimated smooth parameters from datasets corresponding to each accession and each experiment (Supplemental Table S6). Finally, we estimated SPA using the six steps of the statistical model (Table 1), the smooth parameters estimated for each accessions and the initial NO₃ concentration. The computed SPA values were close to the observed SPA values ($R^2 = 0.55$), supporting the idea that the model simulated well the process of NUE in the studied plants.

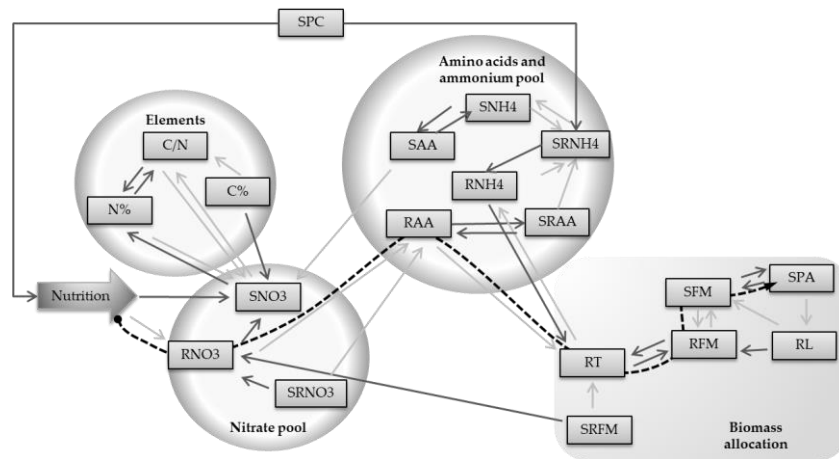


Figure 8. Descriptive model of morphological and metabolic responses to N nutrition. Traits are linked to each other by strong correlative relationships. Dark and light grey arrows link traits with the first and second highest correlated traits, respectively, according to Pearson’s correlation matrix (Supplemental Table S5). The black dotted line indicates the pathway used in the model to estimate RFM, SFM and SPA from the nutrition regime. Four groups of correlated traits are classified as elements, nitrate pool, free amino acids-ammonium pool, and biomass allocation.

Table 1. Formulas and parameters used by the model to estimate morphological traits according to N nutrition status. In the first three columns, the traits included in the descriptive model are listed, and the formulas and model parameters that fit with all the data. Model parameters refined for each genotype in the three experiments are listed in the Supplemental Table S6.

Model	Formula	Model Parameters	ANOVA		
			Par.	G	E
EnvNO ₃ →RNO ₃	$RNO_3 = A1 \cdot \ln(\text{EnvNO}_3) + A2$	A1 = 60 A2 = 325	A1 A2	* (*)	** **
RNO ₃ →RAA	$RAA = B1 \cdot (RNO_3) + B2$	B1 = 0.018 B2 = 15.87	B1 B2	Ns Ns	(*) (*)
RAA→RT	$RT = C1 \cdot \ln(RAA) + C2$	C1 = 0.58 C2 = 2.51	C1 C2	* **	ns ns
RT→RFM	$RFM = D1 \cdot (RT) + D2$	D1 = 22.14 D2 = -1.76	D1 D2	Ns Ns	ns ns
RFM→SFM	$SFM = E1 \cdot (RFM)^{E2}$	E1 = 11.72 E2 = 0.62	E1 E2	Ns Ns	(*) (*)
SFM→SPA	$SPA = F1 \cdot (SFM) + F2$	F1 = 0.05 F2 = 0.7	F1 F2	Ns Ns	ns ns

Significance of the variation due to genotype (G) and to experience (E) for the refined parameters (Par.) in ANOVA is reported by “***” for highly significant ($p < 0.01$), “**” for significant ($p < 0.05$), “(*)” for nearly significant ($0.05 < p < 0.06$) and “ns” for not significant.

The ANOVA of these smooth parameters allowed to identifying the ones that respond to experimental and/or genotype factors. Significance of experimental and genotype factors for each parameter were displayed in Table 1. The parameters A1 and A2 of the first equation connecting RNO₃ to the NO₃ environment were significantly genotype-dependent (p -value < 0.05 and p -value < 0.06, respectively). In addition, the parameters C1 and C2 in the equation linking RAA to RT were explained by a genotype factor (p -value < 0.05 and p -value < 0.01, respectively). Genetic variation for the A1 parameter revealed a higher and faster nitrate accumulation in roots depending on nutrition regimes in *Col-0* compared to the other accessions. Genetic variation for C1 and C2 parameters revealed a difference in the relationship linking RAA to RT between accessions. Characterized by the highest C1 and C2 values, *Bur-0* was the accession showing the highest increase of its root thickness when RAA decreased. In contrast, following the statistical model, *Col-0* showed the lowest modulation of RT when RAA varied. Significant variation was observed between experiments for A1 and A2 parameters (p -value < 0.01 and p -value < 0.055, respectively), suggesting a continuum environmental differences between experiments.

4. Discussion

Natural variation provides an excellent framework to investigate plant adaptation to simultaneous genetic changes and environmental variations. Plant response to N availability has been widely studied in *Arabidopsis* as well as in crop species, most often focusing only on ample, limiting, and scarcity conditions [14,16,19,37,38]. With this study, we quantified the *Arabidopsis* response to an ample set of nutrition regimes, ranging from 0.01 mM up to 50 mM NO₃, taking into account genotype features. We investigated both induced increases and decreases of N concentration compared to a control nutrition regime, a likely scenario that describes what plants face in an agricultural context. This allowed an accurate description of the dynamics of N pools (total N%, NO₃ pools, free amino acid and ammonium pools) and the formulation of a statistic model to correlate nutrition-responsive traits in *Arabidopsis*.

The present study gives the global response of *Arabidopsis* to a wide range of N regimes, computed from the average of contrasted genotypes, and completes some previous studies [13–16]. We observed first that the expected positive correlation existing between NO₃ abundance in media and certain metabolic traits such as the total N percentage and free amino acid content [13,15] was only partially confirmed in our study. Total N percentage indeed remained substantially stable from 0.2 mM to 50 mM nutrition, while we clearly observed an increase of nitrate, amino acids, and ammonium in both shoots and roots towards the highest NO₃ media concentrations (Figure 3). The break happens when total N percentage decreases under the critical N value (the amount of supplied nitrogen beyond which plants stop biomass production). This threshold is reached when the external NO₃ is between 0.2 mM and 1 mM in *Arabidopsis* (Figure 6). We observed a decrease of protein content in shoots (SPC) under both low and high nutrition regimes (Figure 3). This result is in contrast with previous descriptions [10,13,15] where no changes were detected between low and high N regimes for SPC. We hypothesized a change in the dynamics of N pools when the plants are growing at high NO₃ concentrations. Total N percentage remains stable, but the amount of proteins decreases in favor of accumulation of free amino acids, ammonium, and nitrate. A negative impact at extreme NO₃ concentrations was remarked in our investigation on shoot biomass, a trait which is usually known to be highly impacted by N scarcity [16,18,39]. A decrease in SFM was expected and found at a NO₃ availability lower than the control. In this case, all N-related traits decreased, due the scarcity of the N resource. Interestingly, we also detected a clear decrease of shoot biomass at high NO₃ concentrations, in which plants dispose of excess amounts of NO₃. This may represent a symptom of impairment of carbon inclusion in the GS/GOGAT cycle to form amino acids. Indeed, plant growth and development are highly dependent on the interaction between C and N metabolism [40]. As large amounts of N are invested in the photosynthetic machinery, optimal CO₂ assimilation through photosynthesis and, as a consequence, biomass production requires an adequate N supply. On the other hand, it has also been

long established that during the assimilation of inorganic N, significant amounts of fixed C are required to provide the C skeletons that act as acceptors during N assimilation and use, and significant amounts of ATP and NAD(P)H are required to drive these processes. At very high NO₃ media availability, plants continue to uptake N, and they stock it in vacuoles, reaching very high N concentrations [41]. However, we have evidence that increases in shoot biomass become impossible in this case, and at the same time, carbohydrates are driven towards starch production. SStarch was indeed extremely increased at low N regimes, confirming the well-known response to N starvation [16,19,42], but it was also accumulated at high N regimes, where it accompanied the decrease of SFM (Figure 2). Starch, if incompletely remobilized, can therefore sequester carbon that could otherwise be invested in leaf and root growth [42]. To some extent we found the usual attempt of plants to scavenge for nutrients at low NO₃ supplies [11], with a slight increase of RFM essentially due to lateral roots emergence and increase of their architecture complexity. We could in fact even detect a decrease of primary root length in all nutrient regimes compared to control, while root thickness was increased at the lowest supply and decreased at the highest NO₃ supply (Figure 2).

Our investigation provides a statistical model to estimate biomass allocation from the initial NO₃ availability, taking in account the genotype specificities. From the correlation analysis, we can notice that shoot biomass and other morphological traits are more connected to root metabolic traits than to shoot metabolic traits (Figure 8). RT plays a key role in connecting the group of amino acids and ammonium pools to the group of biomass traits. It represents the size and architecture of secondary roots. The negative correlation between RAA and RT was strong in all experiments and for all genotypes. It suggests that plants that present a low level of free amino acids in roots, are able to acquire a higher root biomass or vice-versa, and consequently support the growth of aerial parts, since RFM and SFM are positively correlated to RT. Indeed, *Col-0* is the only genotype that presented a higher RAA content in all conditions compared to control, and did not increase its root size or root architecture shape to respond to N limitation. This is in agreement with results from Krapp et al. [8] that detected stable levels of root amino acids after several days of N shortage accompanied by huge secondary root development in *Col-0*. In contrast, other studies stated that RAA and RT have a positive correlation in limiting N in several accessions [16] and some genotypes that better resist an N-perturbed environment are characterized by a stronger accumulation of RAA and RFM compared to sensitive lines [15]. The negative correlation reported here might have arisen because of the wider range of N supplies in which plants have been grown. RAA has a negative correlation with RNO₃ and a positive one with SRNO₃ (Table S3), suggesting that the key for adaptation to N stress is the ability of a plant to transport NO₃ towards shoots where it will be reduced and assimilated into amino acids, avoiding RNO₃ accumulation [43]. Starch is described by Calenge et al. [39] as a likely contributor to dry matter accumulation according to the positive correlation between these two traits both in normal and limiting N supplies, but the present study revealed a negative correlation between SStarch and SFM (data not shown). With extreme supplies of 0.01 mM and 50 mM NO₃, conditions in which plants undergo a sensitive decrease in SFM, we could indeed observe a significant increase in SStarch, suggesting that starch accumulation may not be a specific response to low N availability but rather a plant response to nutrient conditions unsuitable for optimal growth.

Our study gives some clues on the strategies used by plants when faced with a N stress environment. The four accessions used in our investigation have been previously classified according to their different reactions to N limitations [16]. Briefly, *Bur-0* was described as an accession well adapted to N limitation. *Ge-0* belonged to a group of accessions which supported a complete N starvation. *Cvi-0* was an accession less adapted to N limitation and *Col-0* showed a low growth and a low adaptation to N stress. In the present study, we characterized the response of these four accessions to different N stress environments. Evaluating the status of the different N pools in plants, we showed that the accessions varied for their different nutrition indexes (NNI, NO₃NI and AANI). NNI stayed high in *Cvi-0* growing in low or high NO₃ concentrations, whereas the index decreased in the three other accessions (Figure 6). This means that the N pools stay filled in this accession, even under N

stress conditions. This result suggested that *Cvi-0* is relatively insensitive to N availability. Its weak response might explain why this genotype is less adapted to N limitation [16]. The shoot biomass (SFM) was positively correlated to NNI (Figure 7). The estimation of the slope of the regression line for each genotype revealed genetic specificities. The slopes of the regression line were high in *Bur-0*, intermediate in *Cvi-0* and *Ge-0*, and low in *Col-0*, indicating that the biomass produced at the same NNI will be higher in *Bur-0* than in *Col-0*, and revealing a higher NUE in *Bur-0* than in *Col-0*. These differences in NUE are congruent with previous observations [15,16,19]. Finally, a genetic variation was observed for the relationship connecting amino acid content in roots, RAA, and root thickness, RT (Table 1). In the highly efficient accession *Bur-0*, the two root traits are well opposed; the reduction of amino acids in roots is associated with a development of root architecture. In contrast, RAA remains high and RT varied slightly in the poorly efficient accession *Col-0*. Taking together, the results suggest that the capacity of the plant to transform amino acids into secondary and lateral roots is an interesting and surprising part of NUE in plants.

Supplementary Materials: The following are available online at <http://www.mdpi.com/2077-0472/8/2/28/s1>, Table S1: Raw dataset corresponding to all measurements made on four *Arabidopsis* accessions in six N supplies for three independent experiments, Table S2: Percentage of explained variance of investigated traits, Table S3: Nutrition indexes of different N pools in the four *Arabidopsis* accessions, Table S4: ANOVA of the five nutrition indexes in four *Arabidopsis* accessions growing in six different N supplies in three independent experiments., Table S5: Pearson's correlation matrix of investigated traits, Table S6: Parameters of the descriptive model for the estimation of morphological traits according to N nutrition, Figure S1: Slope (A) and intercept (B) of linear regression of SFM against NNI for the 4 *Arabidopsis* accessions, Figure S2: Nutrition Use Efficiency in four *Arabidopsis* accessions.

Acknowledgments: We thank David Lawrence for English editing this work was supported by the Marie Curie Initial Training Network, project No 264296, BIONUT. The IJPB benefits from the support of the LabEx Saclay Plant Sciences-SPS (ANR-10-LABX-0040-SPS).

Author Contributions: F.C. and S.C. conceived and designed the experiments; G.C. and F.C. performed the experiments; G.C., C.M.-D. and F.C. analyzed the data; M.B. and A.M. contributed reagents/materials/analysis tools; G.C. and F.C. wrote the paper.

Conflicts of Interest: The authors declare no conflict of interest.

References

1. Bouguyon, E.; Gojon, A.; Nacry, P. Nitrate sensing and signaling in plants. *Semin. Cell Dev. Biol.* **2012**, *23*, 648–654. [[CrossRef](#)] [[PubMed](#)]
2. Diaz, C.; Lemaître, T.; Christ, A.; Azzopardi, M.; Kato, Y.; Sato, F.; Morot-Gaudry, J.-F.; Le Dily, F.; Masclaux-Daubresse, C. Nitrogen recycling and remobilization are differentially controlled by leaf senescence and development stage in *Arabidopsis* under low nitrogen nutrition. *Plant Physiol.* **2008**, *147*, 1437–1449. [[CrossRef](#)] [[PubMed](#)]
3. Kant, S.; Bi, Y.M.; Rothstein, S.J. Understanding plant response to nitrogen limitation for the improvement of crop nitrogen use efficiency. *J. Exp. Bot.* **2011**, *62*, 1499–1509. [[CrossRef](#)] [[PubMed](#)]
4. Masclaux-Daubresse, C.; Chen, Q.; Havé, M. Regulation of nutrient recycling via autophagy. *Curr. Opin. Plant Biol.* **2017**, *39*, 8–17. [[CrossRef](#)] [[PubMed](#)]
5. Kim, J.; Woo, H.R.; Nam, H.G. Toward systems understanding of leaf senescence: An integrated multi-omics perspective on leaf senescence research. *Mol. Plant* **2017**, *9*, 813–825. [[CrossRef](#)] [[PubMed](#)]
6. Tegeder, M.; Masclaux-Daubresse, C. Source and sink mechanisms of nitrogen transport and use. *New Phytol.* **2018**, *217*, 35–53. [[CrossRef](#)] [[PubMed](#)]
7. De Pessemier, J.; Chardon, F.; Juraniec, M.; Delaplace, P.; Hermans, C. Natural variation of the root morphological response to nitrate supply in *Arabidopsis thaliana*. *Mech. Dev.* **2013**, *130*, 45–53. [[CrossRef](#)] [[PubMed](#)]
8. Krapp, A.; Berthomé, R.; Orsel, M.; Mercey-Boutet, S.; Yu, A.; Castaigns, L.; Elftieh, S.; Major, H.; Renou, J.-P.; Daniel-Vedele, F. *Arabidopsis* roots and shoots show distinct temporal adaptation patterns toward nitrogen starvation. *Plant Physiol.* **2011**, *157*, 1255–1282. [[CrossRef](#)] [[PubMed](#)]

9. Krapp, A.; David, L.C.; Chardin, C.; Girin, T.; Marmagne, A.; Leprince, A.S.; Chaillou, S.; Ferrario-Méry, S.; Meyer, C.; Daniel-Vedele, F. Nitrate transport and signalling in arabidopsis. *J. Exp. Bot.* **2014**, *65*, 789–798. [[CrossRef](#)] [[PubMed](#)]
10. Lemaître, T.; Gaufichon, L.; Boutet-Mercey, S.; Christ, A.; Masclaux-Daubresse, C. Enzymatic and metabolic diagnostic of nitrogen deficiency in *Arabidopsis thaliana* Wassilewskija accession. *Plant Cell Physiol.* **2008**, *49*, 1056–1065. [[CrossRef](#)] [[PubMed](#)]
11. Walch-Liu, P.; Ivanov, I.I.; Filleur, S.; Gan, Y.B.; Remans, T.; Forde, B.G. Nitrogen regulation of root branching. *Ann. Bot.* **2006**, *97*, 875–881. [[CrossRef](#)] [[PubMed](#)]
12. Loudet, O.; Chaillou, S.; Camilleri, C.; Bouchez, D.; Daniel-Vedele, F. Bay-0 x Shahdara recombinant inbred line population: A powerful tool for the genetic dissection of complex traits in *Arabidopsis*. *Theor. Appl. Genet.* **2002**, *104*, 1173–1184. [[CrossRef](#)] [[PubMed](#)]
13. Loudet, O.; Chaillou, S.; Merigout, P.; Talbotec, J.; Daniel-Vedele, F. Quantitative trait loci analysis of nitrogen use efficiency in *Arabidopsis*. *Plant Physiol.* **2003**, *131*, 345–358. [[CrossRef](#)] [[PubMed](#)]
14. North, K.A.; Ehlting, B.; Koprivova, A.; Rennenberg, H.; Kopriva, S. Natural variation in *Arabidopsis* adaptation to growth at low nitrogen conditions. *Plant Physiol. Biochem.* **2009**, *47*, 912–918. [[CrossRef](#)] [[PubMed](#)]
15. Richard-Molard, C.; Krapp, A.; Brun, F.; Ney, B.; Daniel-Vedele, F.; Chaillou, S. Plant response to nitrate starvation is determined by N storage capacity matched by nitrate uptake capacity in two *Arabidopsis* genotypes. *J. Exp. Bot.* **2008**, *59*, 779–791. [[CrossRef](#)] [[PubMed](#)]
16. Ikram, S.; Bedu, M.; Daniel-Vedele, F.; Chaillou, S.; Chardon, F. Natural variation of *Arabidopsis* response to nitrogen availability. *J. Exp. Bot.* **2012**, *63*, 91–105. [[CrossRef](#)] [[PubMed](#)]
17. Peng, M.; Hudson, D.; Schofield, A.; Tsao, R.; Yang, R.; Gu, H.; Bi, Y.M.; Rothstein, S.J. Adaptation of *Arabidopsis* to nitrogen limitation involves induction of anthocyanin synthesis which is controlled by the NLA gene. *J. Exp. Bot.* **2008**, *59*, 2933–2944. [[CrossRef](#)] [[PubMed](#)]
18. Chardon, F.; Noël, V.; Masclaux-Daubresse, C. Exploring NUE in crops and in *Arabidopsis* ideotypes to improve yield and seed quality. *J. Exp. Bot.* **2012**, *63*, 3401–3412. [[CrossRef](#)] [[PubMed](#)]
19. Chardon, F.; Barthélémy, J.; Daniel-Vedele, F.; Masclaux-Daubresse, C. Natural variation of nitrate uptake and nitrogen use efficiency in *Arabidopsis thaliana* cultivated with limiting and ample nitrogen supply. *J. Exp. Bot.* **2010**, *61*, 2293–2302. [[CrossRef](#)] [[PubMed](#)]
20. Sulpice, R.; Nikoloski, Z.; Tschoep, H.; Antonio, C.; Kleessen, S.; Larhlimi, A.; Selbig, J.; Ishihara, H.; Gibon, Y.; Fernie, A.R.; et al. Impact of the carbon and nitrogen supply on relationships and connectivity between metabolism and biomass in a broad panel of *Arabidopsis* Accessions. *Plant Physiol.* **2013**, *162*, 347–363. [[CrossRef](#)] [[PubMed](#)]
21. Chietera, G.; Chardon, F. Natural variation as a tool to investigate nutrient use efficiency in plants. In *Nutrient Use Efficiency in Plants: Concepts and Approaches*; Hawkesford, M.J., Kopriva, S., De Kok, L.J., Eds.; Springer International Publishing: Cham, Switzerland, 2014; pp. 29–50.
22. Weigel, D. Natural variation in *Arabidopsis*: From molecular genetics to ecological genomics. *Plant Physiol.* **2012**, *158*, 2–22. [[CrossRef](#)] [[PubMed](#)]
23. Sinclair, T.R.; Purcell, L.C.; Sneller, C.H. Crop transformation and the challenge to increase yield potential. *Trends Plant Sci.* **2004**, *9*, 70–75. [[CrossRef](#)] [[PubMed](#)]
24. Picheny, V.; Casadebaig, P.; Trépos, R.; Faivre, R.; Da Silva, D.; Vincourt, P.; Costes, E. Using numerical plant models and phenotypic correlation space to design achievable ideotypes. *Plant Cell Environ.* **2017**, *40*, 1926–1939. [[CrossRef](#)] [[PubMed](#)]
25. Boote, K.J.; Jones, J.W.; White, J.W.; Asseng, S.; Lizaso, J.I. Putting mechanisms into crop production models. *Plant Cell Environ.* **2013**, *36*, 1658–1672. [[CrossRef](#)] [[PubMed](#)]
26. Stewart, D.W.; Cober, E.R.; Bernard, R.L. Modeling genetic effects on the photothermal response of soybean phenological development. *Agron. J.* **2003**, *95*, 65–70. [[CrossRef](#)]
27. Reymond, M.; Muller, B.; Leonardi, A.; Charcosset, A.; Tardieu, F. Combining quantitative trait Loci analysis and an ecophysiological model to analyze the genetic variability of the responses of maize leaf growth to temperature and water deficit. *Plant Physiol.* **2003**, *131*, 664–675. [[CrossRef](#)] [[PubMed](#)]
28. Quilot, B.; Kervella, J.; Génard, M.; Lescouret, F. Analysing the genetic control of peach fruit quality through an ecophysiological model combined with a QTL approach. *J. Exp. Bot.* **2005**, *56*, 3083–3092. [[CrossRef](#)] [[PubMed](#)]

29. Bertin, N.; Martre, P.; Génard, M.; Quilot, B.; Salon, C. Under what circumstances can process-based simulation models link genotype to phenotype for complex traits? Case-study of fruit and grain quality traits. *J. Exp. Bot.* **2010**, *61*, 955–967. [[CrossRef](#)] [[PubMed](#)]
30. Salon, C.; Lepetit, M.; Gamas, P.; Jeudy, C.; Moreau, S.; Moreau, D.; Voisin, A.S.; Duc, G.; Bourion, V.; Munier-Jolain, N. Analysis and modeling of the integrative response of *Medicago truncatula* to nitrogen constraints. *C. R. Biol.* **2009**, *332*, 1022–1033. [[CrossRef](#)] [[PubMed](#)]
31. Gu, J.; Yin, X.; Zhang, C.; Wang, H.; Struik, P.C. Linking ecophysiological modelling with quantitative genetics to support marker-assisted crop design for improved yields of rice (*Oryza sativa*) under drought stress. *Ann. Bot.* **2014**, *114*, 499–511. [[CrossRef](#)] [[PubMed](#)]
32. Martre, P.; Porter, J.R.; Jamieson, P.D.; Triboï, E. Modeling grain nitrogen accumulation and protein composition to understand the sink/source regulations of nitrogen remobilization for wheat. *Plant Physiol.* **2003**, *133*, 1959–1967. [[CrossRef](#)] [[PubMed](#)]
33. Miranda, K.M.; Espey, M.G.; Wink, D.A. A rapid, simple spectrophotometric method for simultaneous detection of nitrate and nitrite. *Nitric Oxide* **2001**, *5*, 62–71. [[CrossRef](#)] [[PubMed](#)]
34. Rosen, H. A modified ninhydrin colorimetric analysis for amino acids. *Arch. Biochem. Biophys.* **1957**, *67*, 10–15. [[CrossRef](#)]
35. Lemaire, G.; Jeuffroy, M.-H.; Gastal, F. Diagnosis tool for plant and crop N status in vegetative stage: Theory and practices for crop N management. *Eur. J. Agron.* **2008**, *28*, 614–624. [[CrossRef](#)]
36. Cohen, J.; Cohen, P.; West, S.G.; Aiken, L.S. *Applied Multiple Regression/Correlation Analysis for the Behavioral Sciences*, 3rd ed.; Laurence Erlbaum Associates, Inc.: Mahwah, NJ, USA, 2003.
37. Cañas, R.A.; Yesbergenova-Cuny, Z.; Simons, M.; Chardon, F.; Armengaud, P.; Quilleré, I.; Cukier, C.; Gibon, Y.; Limami, A.M.; Nicolas, S.; et al. Exploiting the genetic diversity of maize using a combined metabolomic, enzyme activity profiling, and metabolic modelling approach to link leaf physiology to kernel yield. *Plant Cell* **2017**, *29*, 919–943. [[CrossRef](#)] [[PubMed](#)]
38. Dai, Z.; Plessis, A.; Vincent, J.; Duchateau, N.; Besson, A.; Dardevet, M.; Prodhomme, D.; Gibon, Y.; Hilbert, G.; Pailloux, M.; et al. Transcriptional and metabolic alternations rebalance wheat grain storage protein accumulation under variable nitrogen and sulfur supply. *Plant J.* **2015**, *83*, 326–343. [[CrossRef](#)] [[PubMed](#)]
39. Calenge, F.; Saliba-Colombani, V.; Mahieu, S.; Loudet, O.; Daniel-Vedele, F.; Krapp, A. Natural variation for carbohydrate content in *Arabidopsis*. Interaction with complex traits dissected by quantitative genetics. *Plant Physiol.* **2006**, *141*, 1630–1643. [[CrossRef](#)] [[PubMed](#)]
40. Nunes-Nesi, A.; Fernie, A.R.; Stitt, M. Metabolic and signaling aspects underpinning the regulation of plant carbon nitrogen interactions. *Mol. Plant* **2010**, *3*, 973–996. [[CrossRef](#)] [[PubMed](#)]
41. De Angeli, A.; Monachello, D.; Ephritikhine, G.; Frachisse, J.M.; Thomine, S.; Gambale, F.; Barbier-Brygoo, H. The nitrate/proton antiporter AtCLCa mediates nitrate accumulation in plant vacuoles. *Nature* **2006**, *442*, 939. [[CrossRef](#)] [[PubMed](#)]
42. Stitt, M.; Zeeman, S.C. Starch turnover: Pathways, regulation and role in growth. *Curr. Opin. Plant Biol.* **2012**, *15*, 282–292. [[CrossRef](#)] [[PubMed](#)]
43. Masclaux-Daubresse, C.; Daniel-Vedele, F.; Dechorgnat, J.; Chardon, F.; Gaufichon, L.; Suzuki, A. Nitrogen uptake, assimilation and remobilization in plants: Challenges for sustainable and productive agriculture. *Ann. Bot.* **2010**, *105*, 1141–1157. [[CrossRef](#)] [[PubMed](#)]

